Level-crossing study of the hyperfine structure of lithium

W. Nagourney† and W. Happer
Columbia Radiation Laboratory, Department of Physics, Columbia University, New York, New York 10027
A. Lurio
IBM Research Center, Box 218, Yorktown Heights, New York 10598

(Received 28 November 1977)

The method of level-crossing spectroscopy has been employed to measure the hyperfine interaction constants and the lifetimes of the $2\,^2P$ and $3\,^2P$ states of ^{7}Li. The parameters for the $P_{3/2}$ states were obtained from a conventional level-crossing experiment; it was also possible to measure the magnetic dipole hyperfine structure constant A for $P_{1/2}$ states by using a newer method (similar to level crossing) called the "decoupling" method. With these techniques, it was possible to measure A for the $2\,^2P_{3/2}$, $3\,^2P_{3/2}$, and $3\,^2P_{1/2}$ states of ^{7}Li. These measurements, together with the measurement of B for the $3\,^2P_{3/2}$ state, made it possible to infer the nuclear quadrupole moment of ^{7}Li. In order to check the consistency of the A values obtained from the decoupling runs, data were taken (using the decoupling method) for A for the $2\,^2P_{1/2}$ and $3\,^2P_{1/2}$ states of ^{6}Li. In addition to the hyperfine data, the lifetimes for the $2\,^2P$ and $3\,^2P$ states were also obtained. The results are: $A_{3/2}(^7\text{Li}\ 2\,^2P) = -2.95(4)$ MHz, $A_{3/2}(^7\text{Li}\ 3\,^2P) = -1.036(16)$ MHz, $A_{1/2}(^7\text{Li}\ 3\,^2P) = 13.7(12)$ MHz, $A_{1/2}(^6\text{Li}\ 3\,^2P) = 5.3(4)$ MHz, $A_{1/2}(^6\text{Li}\ 2\,^2P) = 17.8(3)$ MHz, $B(^7\text{Li}\ 3\,^2P) = -0.094(10)$ MHz, $\tau(2\,^2P) = 26.4(8)$ nsec, $\tau(3\,^2P) = 203(8)$ nsec, and $Q(^7\text{Li}) = -59(8)$ mb.

I. INTRODUCTION

The level-crossing method of optical spectroscopy is one of the major means by which certain properties of excited states of atoms (and molecules) are measured. This technique, along with that of optical double resonance, has certain significant advantages over previous methods of measuring atomic properties. First, since level crossing does not involve the direct measurement of an optical wavelength, the Doppler-width limitation of conventional optical spectroscopy does not apply. Second, the method is applicable to excited states. Third, for well-resolved crossings, the precision of the measurements is in principle limited only by the finite lifetime of the excited state.

We have used this technique to measure the magnetic dipole interaction constant A for the $2\,^2P_{3/2}$ and $3\,^2P_{3/2}$ states and the electric quadrupole constant B for the $3\,^2P_{3/2}$ state of ^{7}Li. A related method, called the "decoupling" method, was used to measure A for the $3\,^2P_{1/2}$ state of ^{7}Li and the $2\,^2P_{1/2}$ and $3\,^2P_{1/2}$ states of ^{6}Li. We have also been able to measure, using the level-crossing method, the lifetimes for the $2\,^2P$ and $3\,^2P$ states of ^{7}Li. Our initial motivation in making these measurements was to compare our values of the magnetic dipole hyperfine interaction constants for the $2\,^2P$ and $3\,^2P$ states of ^{7}Li with the results of numerous theoretical calculations[1-10] carried out using a variety of methods. Such comparisons are of interest because lithium is the simplest atom which exhibits the exchange polarization of the closed-shell core electrons with the valence electron. Furthermore, there is good reason to expect that the contribution to the magnetic dipole hyperfine interaction from core polarization is larger in lithium than in any other alkali atom. From our measurement of B for the $3\,^2P_{3/2}$ state of ^{7}Li we were able to infer a value of the nuclear quadrupole moment Q which is difficult to obtain from the $2\,^2P$ state. Our result might be helpful in resolving the question of the size of the Sternheimer correction to the electric quadrupole interaction.

The chief problem in using the level-crossing method to measure the hyperfine structure (hfs) of lithium is that, for the first excited state of ^{7}Li, the crossings are not resolved at all; and, for the second excited state, they are only poorly resolved. A useful rule of thumb is that for the crossings to be well resolved, the product of the lifetime in nanoseconds and the magnetic hyperfine interaction constant A in megahertz should be greater than 100. For the $2\,^2P_{3/2}$ state of ^{7}Li, this product is about 81, and for the $3\,^2P_{3/2}$ state it is approximately 200. Since there are no resolvable crossings in the first state, the data analysis necessitates a computer fit of the theoretical curves of scattered intensity versus magnetic field to the experimental curves.

Two other problems made this experiment somewhat more difficult than most conventional level-crossing measurements. The first is the extreme reactivity of lithium when hot. Because of this, it was considered desirable to use an atomic beam in the scattering region, rather than a cell. Cells with MgO windows can be used but are extremely awkward to construct. Furthermore, the reactivity of lithium necessitated the use of a flow lamp as the source of exciting radiation for the cases (the $3\,^2P$-state data) where high intensity was required. The instabilities of this lamp were

never completely eliminated and made it difficult to run for long periods. The second problem was a direct consequence of using an atomic beam rather than a cell: For our 3^2P-state runs, we had considerable difficulty in obtaining more than a marginal signal to background ratio. This problem was due to insufficient Li vapor density in the beam and would have been eliminated if we could have used a cell. The problem was particularly acute for our $3^2P_{1/2}$-state decoupling data, since the amount of scattered light was somewhat smaller for the decoupling data than it was for the level-crossing data.

II. THEORY

A. Resonance fluorescence

The method of level-crossing spectroscopy exploits the interference that occurs when two states are coherently excited by the same photon. If the relative phase of these coherently excited states changes during the time spent in the excited state, the emitted photon which arises from the decay of these states can have a different spatial distribution than that of the exciting photon. This process is quantitatively described by the Breit formula[11,12]

$$I \propto \sum_{\mu,\mu',m,m'} \frac{f_{\mu m} f_{m\mu'} g_{\mu' m'} g_{m'\mu}}{\Gamma - i(E_\mu - E_{\mu'})/\hbar} , \tag{1}$$

where $f_{\mu m} = \langle \mu | \vec{f} \cdot \vec{r} | m \rangle$ and $g_{\mu' m} = \langle \mu' | \vec{g} \cdot \vec{r} | m \rangle$. The vectors $\vec{f}$ and $\vec{g}$ are the polarization vectors for the exciting and scattered radiation, respectively, m and m' refer to the ground state, μ and μ' refer to the excited state, and Γ is the average decay rate per second for the excited-state sublevels. The assumptions for which Eq. (1) hold are that the spectral profile of the exciting light is broad compared to the absorption profile of the fluorescing atoms, the rate of excitation is sufficiently small that stimulated emission can be neglected, and multiple scattering of the absorbed and emitted photons does not occur.

Two interesting effects are described by Eq. (1). The first is the conventional level-crossing effect which occurs when one observes the reradiation from two degenerate or nearly degenerate states which were excited from the same ground state. For resolved crossings, the shape of the curve of scattered intensity versus magnetic field exhibits Lorentzian or dispersion-shaped resonances which are due to the energy denominator in Eq. (1). In order to observe a resonant signal, the difference in azimuthal quantum numbers, Δm_F between states μ and μ', must be less than or equal to 2. However, the selection rules on Δm_I and Δm_J depend upon whether or not I and J are coupled; if I is decoupled from J, the additional selection rule $\Delta m_I = 0$ must hold. The fact that the selection rule depends upon the degree of coupling between I and J has an interesting consequence. Certain matrix elements in Eq. (1) which are nonzero when I and J are coupled vanish when I is decoupled from J; this effect is independent of the crossing of levels μ and μ' and is herein referred to as the "decoupling effect." This phenomenon will be discussed from another viewpoint below.

Some insight into the interpretation of the fluorescent intensity versus magnetic field curve can be obtained by considering the behavior of the expectation value of $\vec{J}$ in the excited state. The simple case of an excited $P_{1/2}$ state will be considered here. In Ref. 13, it is shown that the fluorescent intensity can be written

$$R \propto \mathrm{Tr}\{\rho_e L\} , \tag{2}$$

where ρ_e is the excited-state density matrix and L is the fluorescent-light operator. For decays from a $P_{1/2}$ state to an $S_{1/2}$ state, L is given by (see Ref. 13)

$$L \propto 1 + 2\vec{J} \cdot \vec{S} , \tag{3}$$

where $\vec{S}$ is the spin of the scattered photon. Substituting Eq. (3) into Eq. (2) and using the fact that the trace of ρ_e with any observable of the excited state yields the expectation value of that observable, one gets

$$R \propto 1 + 2\langle \vec{J} \rangle \cdot \vec{S} . \tag{4}$$

This suggests that the intensity of scattered light with a given (circular) polarization can be interpreted as a measure of the atomic expectation value of $\vec{J}$ in the direction of $\vec{S}$.

Excitation with circularly polarized light will prepare an excited state whose polarization (i.e., $\langle \vec{J} \rangle$) is along the spin of the exciting light.[4] If $\vec{J}$ is coupled to $\vec{I}$, $\vec{J}$ and $\vec{I}$ will both precess about $\vec{F} = \vec{I} + \vec{J}$; the result is that the component of $\vec{J}$ along the direction of the exciting light will be reduced. This reduction will not occur, however, when $\vec{J}$ is decoupled from $\vec{I}$. Hence, by monitoring the excited-state polarization as $\vec{J}$ is progressively decoupled from $\vec{I}$ by an external magnetic field, one can infer the size of the coupling (i.e., A).

If the magnetic field $\vec{H}$ has a component which is perpendicular to $\langle \vec{J} \rangle$, the excited-state polarization $\langle \vec{J} \rangle$ will begin to precess about $\vec{H}$ immediately after excitation. For cases where the precession period $h/g_J \mu_0 H$ is less than the excited-state lifetime τ, the subsequent decay will have an isotropic angular distribution. However, if the precession period is greater than τ, the angular distribution will be nonisotropic. This change in

the angular distribution of the fluorescent light with magnetic field is called the Hanle effect (it is essentially a zero-field level crossing). From the above considerations, it should be clear that the Hanle-effect curves contain information from which one can obtain the lifetime.

B. Hyperfine structure

There are three contributions to the magnetic hyperfine interaction. These are the orbital, the spin dipole, and the contact terms; they are given as follows:

$$H_c = \tfrac{8}{3}\pi g_S \mu_B \vec{\mu}_I \cdot \sum_{i=1}^{3} \vec{s}_i \delta(\vec{r}_i) \quad \text{(contact)}, \tag{5}$$

$$H_d = g_S \mu_B \vec{\mu}_I \cdot \sum_{i=1}^{3} [3(\vec{s}_i \cdot \vec{r}_i)\vec{r}_i - r_i^2 \vec{s}_i] r_i^{-5} \quad \text{(dipole)}, \tag{6}$$

$$H_o = 2 g_L \mu_B \vec{\mu}_I \cdot \sum_{i=1}^{3} \vec{l}_i r_i^{-3} \quad \text{(orbital)}, \tag{7}$$

where μ_B is the Bohr magneton, $\vec{\mu}_I$ is the nuclear magnetic moment, $g_S = 2.0023$, $g_L = 0.9992$, and the summation is over all electron coordinates. Each of these interactions has the form of a scalar product of an operator on the nuclear coordinates with an operator on the electronic coordinates. Thus, with the aid of the Wigner-Eckart theorem, one can write (for a given J)

$$H_o = a_{oJ} \vec{I} \cdot \vec{J}, \quad H_d = a_{dJ} \vec{I} \cdot \vec{J}, \quad H_c = a_{cJ} \vec{I} \cdot \vec{J}. \tag{8}$$

These three operators can be added together to form the total magnetic hfs operator

$$H_m = A_J \vec{I} \cdot \vec{J}, \tag{9}$$

where

$$A_J = a_{oJ} + a_{dJ} + a_{cJ}. \tag{9a}$$

Each of the a's as defined above contains the factor $\langle r^{-3} \rangle$ (the contact term is put into this form for convenience). For a $^2P_{3/2}$ state, the a's appearing in Eq. (8) can be expressed as (neglecting relativity corrections)

$$\begin{aligned} a_c &= -g_S \mu_B (\mu_I / I) \tfrac{1}{3} \langle r^{-3} \rangle_c, \\ a_d &= -g_S \mu_B (\mu_I / I) \tfrac{2}{15} \langle r^{-3} \rangle_d, \\ a_o &= 2 g_L \mu_B (\mu_I / I) \tfrac{2}{3} \langle r^{-3} \rangle_o. \end{aligned} \tag{10}$$

If one takes matrix elements with appropriate configuration mixed wave functions, one finds that $\langle r^{-3} \rangle_o$ does not exactly equal $\langle r^{-3} \rangle_d$. The quantities $\langle r^{-3} \rangle$ must then be interpreted as experimental parameters which give the strength of each interaction; they are no longer exact measures of the inverse cube of the distance of the valence electron to the nucleus (indeed, $\langle r^{-3} \rangle_d$ for the $4\,^2D$ state of ^{87}Rb is negative).[14]

Complete specification of the magnetic hfs requires knowledge of all three parameters. For the $^2P_{1/2}$ and $^2P_{3/2}$ states of ^{7}Li, the following relations can be demonstrated[15]:

$$a_{c1/2} = a_{c3/2}, \quad a_{d1/2} = -10 a_{d3/2}, \quad a_{o1/2} = 2 a_{o3/2}. \tag{11a}$$

Then, using Eq. (9a), one has

$$A_{3/2} = a_{c3/2} + a_{d3/2} + a_{o3/2}$$

and

$$A_{1/2} = -a_{c3/2} - 10 a_{d3/2} + 2 a_{o3/2}. \tag{11b}$$

Equations (11b) are two relationships between the experimentally measured parameters and the a's; determination of the a's requires a third independent relation. The third relation usually involves some parameter that is measured at a large magnetic field where crossings occur between fine-structure levels. One possible relation requires the measurement of the interaction matrix element in the anticrossing between the $m_J = -\frac{3}{2}$ and the $m_J = -\frac{1}{2}$ levels; another involves the average field interval between high-field level crossings. The latter relation is (for ^{7}Li)[15]

$$\tfrac{1}{3} \mu_B (10 g_L + g_S)(\Delta H)_{\text{av}} = -5 a_{d3/2} + 5 a_{o3/2} + a_{c3/2}, \tag{12}$$

where $(\Delta H)_{\text{av}}$ is the average field interval between crossings. Equation (12) is correct to first order in the hyperfine interaction; higher-order corrections are not justified by the precision of the experimental data.

The electric quadrupole interaction can be derived from the classical interaction energy of a charge distribution in an electric field. Transforming to a spherical basis and performing some Racah algebra, the result is

$$H_q = \frac{e^2 q_J Q}{2I(2I-1)J(2J-1)} \times [3(\vec{I} \cdot \vec{J})^2 + \tfrac{3}{2}(\vec{I} \cdot \vec{J}) - \vec{I}^2 \vec{J}^2], \tag{13}$$

where

$$Q = \frac{1}{e} \int_{\text{nucleus}} \rho_n(\vec{r}_n)(3Z_n^2 - r_n^2) dV_n \quad \text{for } m_I = I \tag{14}$$

and

$$q_J = \frac{1}{e} \int_{\text{electrons}} \rho_e(\vec{r}_e) \left(\frac{3Z_e^2 - r_e^2}{r_e^5} \right) dV_e \quad \text{for } m_J = J. \tag{15}$$

The quantity measured in the experiment is B, which is given by

$$B = e^2 Q q_J. \tag{16}$$

For a ^2P state, B is given by (neglecting relativity corrections)

$$B = e^2 Q \tfrac{2}{5} \langle r^{-3} \rangle_q . \quad (17)$$

It should be noted that $\langle r^{-3} \rangle_q$ is also modified by configuration interactions and is not necessarily equal to any of the magnetic $\langle r^{-3} \rangle$ factors.

III. EXPERIMENTAL APPARATUS AND PROCEDURES

Block diagrams depicting the experimental arrangement for the level-crossing and decoupling runs are shown in Figs. 1 and 2, respectively. The apparatus used for the level-crossing runs was quite similar to that used by Schmieder[16]; the main difference was in the type of lamps used to provide the resonance radiation. Polarized resonance radiation was focused on an atomic beam and the light scattered at 90° was passed through an analyzer, interference filter, and light pipe, at the end of which it was detected by an EMI 9558B phototube. The purpose of the light pipe was to allow the phototube to be placed some distance from the magnetic field to avoid magnetic effects on the tube gain; this problem was also reduced by mounting the phototube inside a Mu metal shield. Stops were used in both the input and output optics to confine the incident light to the immediate region of the beam and lessen instrumental scattering. The sweeping magnetic field was provided by a pair of precision Helmholtz coils and the field was oriented at right angles to the plane containing the incident and scattered light wave vectors. The transverse components of Earth's field were cancelled to within 5 mG by two orthogonal sets of Helmholtz coils; this was not necessary for the longitudinal component which was measured before each run and subtracted off during the data analysis. Prior to the data taking, the sweeping coils were calibrated once with a ^{85}Rb magnetometer[17] which gave the field as a function of the current through the coils. During data taking, a precision shunt in series with the coils monitored the current through them; the voltage across the shunt was fed into one input of the signal averager and provided the field data that were used during the data analysis. A repetitive triangular sweeping waveform was generated and used to drive a Kepco BPO-56 programmable power supply which drove the sweeping coils. This type of waveform was chosen primarily in order to conceal unilateral drift in the signal; each sweep consisted of two mirror-symmetric sets of data and the effect of such drift in each half would be opposite.

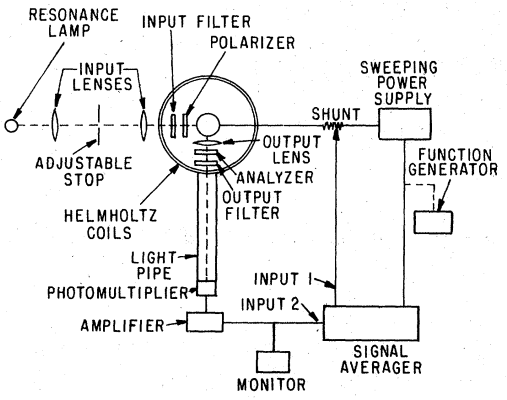

FIG. 1. Schematic diagram of apparatus used in level-crossing experiments. The Li beam is directed out of the plane of the paper in the circle located at the center of the Helmholtz coil.

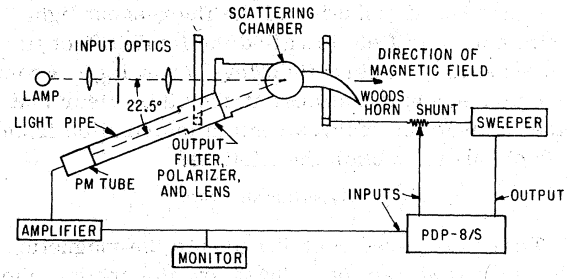

FIG. 2. Schematic diagram of the apparatus used in the decoupling experiments. The Li atomic beam is directed out of the plane of the paper in the center of the region marked scattering chamber. Although not drawn to scale, the sweeping coils have the Helmholtz separation.

The atomic beam was generated in a rectangular stainless-steel oven which was heated by nichrome or tungsten heaters. Nichrome heaters served well for the moderate temperatures required for the $2\,^2P$ states; at 350 °C an adequate beam vapor pressure of 10^{-5} torr was obtained. The $3\,^2P$ states required a beam vapor pressure of about 10^{-3} torr; this was achieved at an oven temperature of 500 °C. At this temperature tungsten heaters were used because they were vastly more reliable. The lithium beam was collimated by an aperture before passing into the scattering region; a beam flag was provided before the aperture to allow one to compare the amount of beam scattering to the instrumental scattering.

A commercially available Perkin Elmer hollow cathode lamp was used as the source of resonance radiation for the $2\,^2P$-state runs; this lamp provided adequate intensity and was exceedingly stable. A flow lamp,[18] however, was needed to excite the $3\,^2P$ states sufficiently. An improved version was used; the major improvement was in the use of external cartridge heaters to generate the lithium beam. With external heaters, it was pos-

sible to avoid the interaction between the heaters and microwaves which led to instabilities in earlier versions of the lamp. This version of the flow lamp was very reliable and fairly stable, but not nearly as stable as the hollow cathode lamp. A cross-sectional view of the improved flow lamp appears in Fig. 3.

The experimental data were acquired and integrated by a 1024-channel analyzer. For some of the data taking, we used a CAT 1000 signal averager; for the rest we used a PDP-8/S which was programmed to behave approximately as a CAT 1000. The main functional difference between these two devices was the way in which the sweeping waveform was generated; when the CAT was used, the sweeping voltage was generated by a HP-202A function generator and synchronization between the CAT and function generator was maintained by the use of the sync pulses provided by the function generator after each cycle. When the PDP-8/S was used, its internal digital to analog converter generated the sweeping voltage directly. A digital signal averager was chosen in preference to a lock-in amplifier mainly because we wanted to avoid the line-shape distortion which might result from magnetic field modulation and phase-sensitive detection with long time constants. Acquiring the data digitally also simplified the transfer of the data to the large computer for analysis.

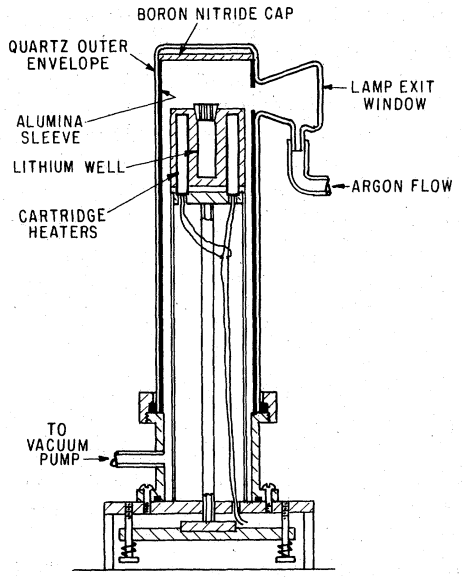

FIG. 3. Modified form of flow lamp used to produce 2^2S to 3^2P radiation. A crinkle-foil top plug on the oven gives a moderately directed lithium beam which is prevented from direct contact with the quartz envelope by means of a removable boron nitride cap. Excitation of the resonance light is provided by a microwave horn located outside the envelope and judiciously placed to optimize intensity and stability. A 100-W Raytheon diathermy unit operating at about 2450 MHz powers this horn.

The decoupling experiments used the same apparatus as was used for the level-crossing runs except for the scattering chamber, which was designed to allow as small an angle as possible between the incident and scattered radiation, since optimum S/N occurs when the incident and detected light beams are either parallel or antiparallel. The angle used was 22.5°. The particular chamber, shown in Fig. 4, also had its windows removed from the near vicinity of the lithium beam to prevent their being coated by hot lithium. Instrumental scattering was reduced by the use of a Wood's horn facing the incident radiation. The sweeping magnetic field used in the decoupling experiments was aligned along the direction of the incident radiation.

The data were analyzed by fitting the experimental points to theoretical curves of scattered intensity versus magnetic field. The theoretical curves depended parametrically on the constants A, B, and lifetime; that set of parameters which gave the best fit (in least-squares sense) was chosen as the result for a given run. Two methods of curve fitting were used. The first, used for the level-crossing data, simply printed out the residual (sum of squared differences) versus the parameter of interest for about ten values around the expected value. The result was obtained by

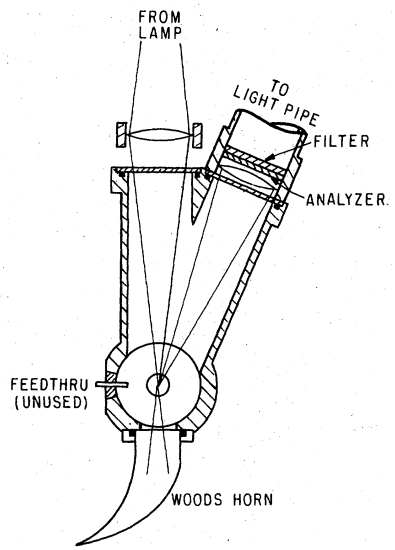

FIG. 4. Details of the apparatus used in the decoupling experiments. The angle between the exciting radiation and the detected radiation is 22.5°.

manually plotting the parabolic-shaped curves of residual versus parameter and taking the value that minimized the residual. In order to avoid recalculation of the theoretical intensities for each run, one set of theoretical curves was generated for a larger than expected range of magnetic field and the Lagrange interpolation method was used to obtain the theoretical points which corresponded to the experimental magnetic field points. The theoretical curves were generated by a program[19] which diagonalizes the hyperfine Hamiltonian to obtain the eigenvalues and eigenvectors and substitutes these into the Breit formula to obtain the scattered intensity. The decoupling data were fitted by a program that automatically searches for a minimum of the residual using the method described by Wentworth.[20] The program recalculates the theoretical intensities several times for each iteration and can be time consuming if the theoretical calculations are complex; hence, it was not used for the level-crossing data. The scattered intensity for the decoupling experiment is described by a rather simple formula [Eq. (18)] and the automatic-curve-fitting program was very suitable for this case. It should be pointed out that, whatever the method used, it was necessary to consider the scale and zero of the experimental points as free parameters since the experiment did not determine them. When the manual-curve-fitting program was used, it was possible to obtain the best-fit scale and zero analytically; with the automatic program, the scale and zero were treated as unknown parameters having the same weight as A and the lifetime.

The running time needed to obtain adequate statistics varied from about 15 min to several hours, depending upon the experimental situation. For the $3^2P_{1/2}$-state decoupling runs, it was necessary to integrate for several hours to obtain marginal data because the scattering from the $3^2P_{1/2}$ state was very small. However, very good data were obtained in about 20 min for the $2^2P_{3/2}$-state level-crossing runs. We found it desirable to break up each running session into several shorter runs between which we would vary some parameter such as the polarization or the oven temperature. This was indispensable in assessing the size and type of systematic error in the experiment. We tried in all cases to analyze the data as soon as possible after the run in order to use the results as a guide to future operating conditions.

IV. SOURCES OF SYSTEMATIC ERRORS

The following sources of systematic errors were taken into account in the experiments. (i) Magnetic field miscalibration. It can be shown that a given fractional error in the magnetic field calibration will produce the same fractional error in the parameters A, B, and τ. This error, which can arise from errors in the original ^{85}Rb magnetometer calibration, error in determining the resistance of the calibration shunt, or errors in the signal averager's analog-to-digital converter was estimated to be less than 0.5%. (ii) Lamp profile. Because of the small (less than 25 MHz) hyperfine intervals and the fairly large[18] (about 4300 MHz for the flow lamp and 2600 MHz for the hollow cathode lamp) estimated Doppler widths of the lamps, any lamp-profile scanning was considered to be completely negligible for the experiments. (iii) Optical alignment. With the geometry used in these experiments, any optical misalignment would destroy the symmetry of the intensity curves about zero field; this was not observed in most runs. However, for some 2^2P-state decoupling runs, a slight asymmetry was observed; readjustment of the optics suggested that the error due to misalignment was less than 1%. (iv) Polarization errors. The polarizers used for the 2^2P-state runs were found to be of very high quality. We do not believe that the lower-quality polarizers used for the 3^2P-state runs have adversly affected the results since the runs taken without polarizers yielded results consistent with those taken with polarizers. Polarizer misalignment would make the intensity curves asymmetric about zero field; this was not observed except for the case mentioned above. (v) Multiple scattering. This could only affect the 2^2P-state results, since the 3^2P-state beam density was not large enough. The results of runs at varied beam oven temperatures do not show any particular trend and multiple scattering was probably not a problem.

V. EXPERIMENTAL RESULTS

In all that follows, the light polarization will be described by two symbols separated by a slash; the first will be the input polarization description and the second will be that of the output. Linear polarization will be described by the angle that the electric field vector of the light makes with the static magnetic field; for example, 0/90 refers to the case where the electric field vector of the incident light is oriented along the direction of the static magnetic field while the field of the scattered light is at right angles to the static field. Circular polarization will be called σ^+ if the transition induced is a $\Delta m = +1$ and σ^- if the transition induced is a $\Delta m = -1$.

The final results for a given parameter were found by making a histogram of the results of all

the individual runs. A bell-shaped error curve was then drawn through the histogram and the value of the parameter was taken as that corresponding to the highest point on the error curve, while the random error was taken as the half width of the curve at half maximum. The final error was obtained by adding in quadrature the random and systematic errors (including the contribution to the random error due to correlations between parameters). This represents a confidence level of greater than 68% (one standard deviation). In all the data analysis, the only data rejections were those made *a priori*, i.e., no data were rejected on the basis of their not yielding results near the average. Data were rejected for some independent reason, such as a magnetic field miscalibration or the presence of a spurious scanning signal.

A. $2\,^2P$ level-crossing data

Level-crossing runs for the $2\,^2P_{3/2}$ state of ^{7}Li were made with 0/0 and 90/90 polarizations. After examining families of theoretical curves for several values of a given parameter, we concluded that the 0/0 polarization should yield the best lifetime data while both polarizations would yield about equally good data for A. The parameter B was considered to be too small compared to A to be measured for the $2\,^2P$ state. The $2\,^2P$-state exciting radiation at 6707 Å was provided by a hollow cathode lamp.

Because of the large absorption cross section for first state resonance radiation, it was necessary to take into account the possibility of multiple scattering of the incident photons. We did this by taking several runs over a range of oven temperatures of from 300 to 500 °C and did not see any systematic trend in the parameters as the oven temperature was increased.

As can be seen in Fig. 5, the curves of scattered intensity for the $2\,^2P_{3/2}$ state were essentially structureless. This made it difficult to obtain two parameters by curve fitting; the best value of one parameter was fairly dependent upon what value the other parameter had during the fitting. We were able to resolve this difficulty by considering the residual versus parameter curves in three dimensions; a parabolic surface was fitted to the residual versus lifetime and A surface, and the adopted result was the value of A and lifetime which corresponded to the lowest point on the surface.

The final results for the $2\,^2P_{3/2}$ level-crossing runs are, for the ^{7}Li $2\,^2P_{3/2}$ state, $A = -2.95 \pm 0.04$ MHz, $\tau = 26.4 \pm 0.8$ nsec.

A fortuitous equality between the fine-structure splitting and the isotope shift (between ^{6}Li and ^{7}Li) made it possible to excite selectively the $P_{1/2}$ state of ^{7}Li with $2\,^2S_{1/2}$ to $2\,^2P_{3/2}$ light from a ^{6}Li hollow cathode lamp; this allowed quite accurate measurement of τ for the $2\,^2P_{1/2}$ state. This could be done since both intervals are about 0.33 Å and the lamp half width profile was about 0.04 Å. Because of the small doublet separation, the $P_{3/2}$ state could not have been eliminated by use of filters. Several runs were taken with circular polarization using the same geometry as for the linear polarization runs and sweeping from about −50 to 50 G. The data (a typical run appears

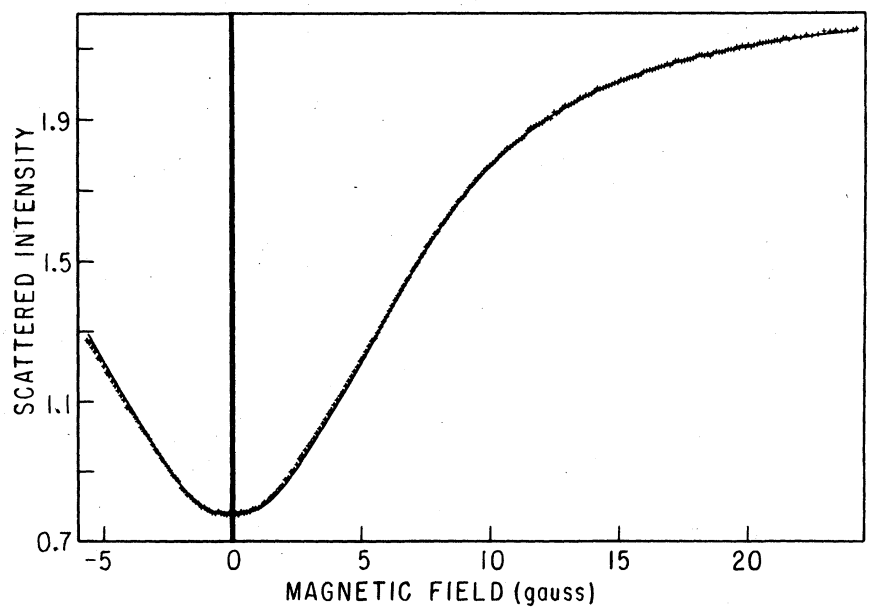

FIG. 5. Level-crossing data for the $2\,^2P$ state. The ×'s are the experimental points and the solid curve is the best-fit theoretical curve. The polarization conditions were 0/0 and the Li atoms were excited with a Perkin Elmer ^{7}Li hollow cathode lamp.

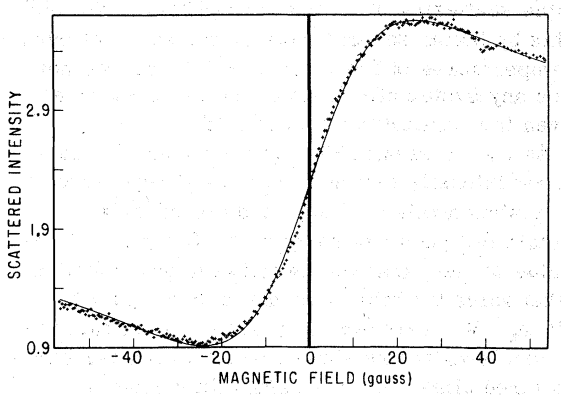

FIG. 6. Level-crossing data taken for the $2\,^2P_{1/2}$ state of ^{7}Li using a Perkin Elmer ^{6}Li hollow cathode lamp and σ^+/σ^+ polarization. Principally the $2\,^2P_{1/2}$ state was excited, but due to the finite spectral width of the ^{6}Li lamp and the presence of ^{7}Li impurities, some small amount of the ^{7}Li $2\,^2P_{3/2}$ state is also excited. The ×'s are the experimental points while the solid line is the optimum computer fit as described in the text.

in Fig. 6) were fitted with the automatic fitting program using the formula, Eq. (18), where A was set at Ritter's[21] value of 46.17 MHz and a variable amount of $J=\frac{3}{2}$ intensities at fixed A and τ were included to account for the possibility of traces of ^{7}Li remaining in the lamp. The average lifetime obtained was, for the ^{7}Li $2\,^2P_{1/2}$ state, $\tau = 26.3 \pm 0.4$ nsec. The error estimate of τ is too large for one to determine whether the difference in τ for the $P_{1/2}$ and $P_{3/2}$ states is real or not.

B. $3\,^2P_{3/2}$ level-crossing data

The $3\,^2P_{3/2}$ level-crossing data were taken with 0/0 and 90/90 polarizations; examination of the theoretical curves showed that the 90/90 polarization would be best for all three parameters. As a check on the quality and alignment of the polarizers, several runs without polarizers were taken; and as shown in Ref. 22, the intensity curve without polarizers is the same as that for the 90/90 polarization. A flow lamp provided $3\,^2P$-state resonance radiation at 3232 Å. The final results are, for the ^{7}Li $3\,^2P_{3/2}$ state, $A = -1.036 \pm 0.016$ MHz; $B = -0.094 \pm 0.010$ MHz; $\tau = 203 \pm 8$ nsec. A typical run appears in Fig. 7.

C. $3\,^2P_{1/2}$ decoupling data

The $3\,^2P_{1/2}$ decoupling data were obtained using both the σ^+/σ^+ polarization and the σ^+/σ^- polarization. The fractional change in the σ^+/σ^+ intensity curves as the magnetic field is swept approaches 1.0, since the observed decays are from an $m_J = -\frac{1}{2}$ state which cannot be populated by a $\Delta m_J = 1$ transition at values of the magnetic field which decouple I and J. Thus, this polarization gives the best signal-to-noise ratio. However, it was useful to take data using both polarizations since the two intensity curves are opposite in sign and possible correlations between the polarization and the results would be a fairly sensitive test of the presence of a spurious scanning signal.

Because of the small splitting between the $3\,^2P_{3/2}$ state and the $3\,^2P_{1/2}$ state, the presence of the $P_{3/2}$ signal had to be taken into account. One approach was to start the sweep at a magnetic field at which the $P_{3/2}$ signal was already at its high-field asymptote (taking advantage of the fact that A for the $P_{3/2}$ state is much smaller than A for the $P_{1/2}$ state). Another approach was to include a variable amount of $P_{3/2}$ intensities for a fixed A and τ in the fitting program. Both approaches were used and yielded very nearly the same results.

As a self-consistency check of the data, runs were made for both isotopes; the resulting values of A should scale exactly as μ_N/I. The results are, for the ^{7}Li $3\,^2P_{1/2}$ state, $A = 13.7 \pm 1.2$ MHz; and for the ^{6}Li $3\,^2P_{1/2}$ state, $A = 5.3 \pm 0.4$ MHz. The experimental ratio of $A(^6\text{Li})$ to $A(^7\text{Li})$ for the $3\,^2P_{1/2}$ state is 0.387 ± 0.04; this compares well with the actual ratio, 0.376, of μ_N/I for the two isotopes. Typical runs for ^{7}Li and ^{6}Li are shown in Figs. 8 and 9, respectively.

As an additional check of the decoupling method, we used it to find A for the $2\,^2P_{1/2}$ state of ^{6}Li; results by other investigators have already been published with which we could compare our results. A typical run is shown in Fig. 10 and the results are, for the ^{6}Li $2\,^2P_{1/2}$ state, $A = 17.9$

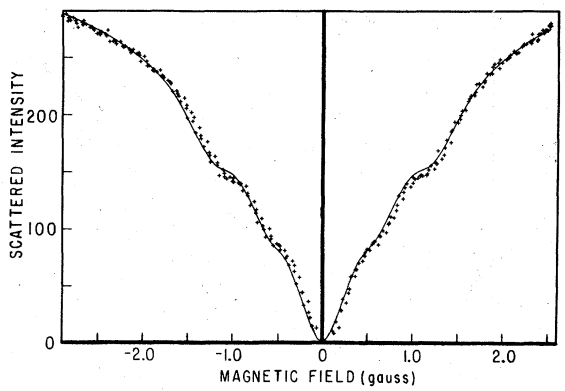

FIG. 7. Level-crossing data taken for the $3\,^2P_{3/2}$ state of ^{7}Li using a flow lamp for excitation. Two inflection points are clearly visible indicating the regions where partially resolved level crossings occur. The crosses are the experimental points and the solid line is the best theoretical fit. The polarization was 90/90.

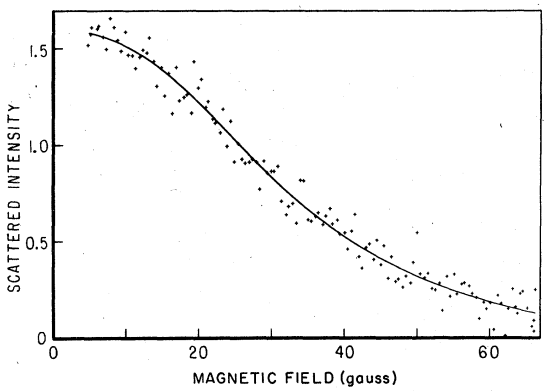

FIG. 8. Decoupling data for the $3\,^2P_{1/2}$ state of ^{7}Li. The crosses are the experimental points and the solid line is the best fit curve. The polarization was σ^+/σ^+ and the source of resonance radiation was the flow lamp.

± 0.35 MHz. This result compares reasonably with Ritter's[21] value of 17.48 ± 0.15 MHz, as the two experimental results lie within their combined error.

D. Derived magnetic hyperfine parameters

As discussed in Sec. II, the interaction constants a_o, a_d, and a_c can be determined if three particular experimental parameters are measured. Our experiments measured $A_{1/2}$ and $A_{3/2}$ for the $3\,^2P$ state and $A_{3/2}$ for the $2\,^2P$ state of ^{7}Li. These results can be combined with the Orth *et al.*[25] value of $A_{1/2}$ and the Brog *et al.*[23] value of $(\Delta H)_{av}$ [see Eq. (11)] for the $2\,^2P$ state of ^{7}Li and the measurement by Isler *et al.*[24] of $(\Delta H)_{av}$ for the $3\,^2P$ state of ^{7}Li to obtain all of the interaction constants for the $2\,^2P$ and $3\,^2P$ states of ^{7}Li. These experimental quantities will be substituted into Eqs. (11b) and (12) to obtain the desired results.

For the $2\,^2P$ state of ^{7}Li, the experimental parameters are $A_{3/2} = -2.95 \pm 0.04$ MHz (this work),

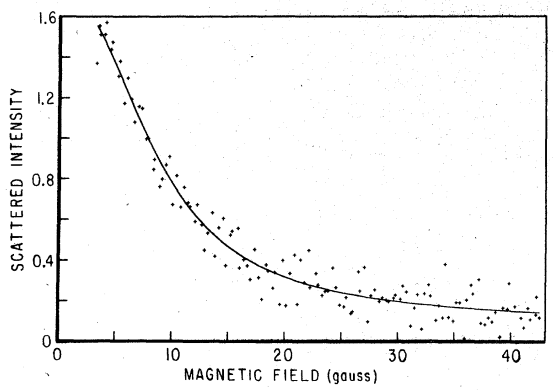

FIG. 9. Decoupling data for the $3\,^2P_{1/2}$ state of ^{6}Li using σ^+/σ^+ polarization and the flow lamp for excitation.

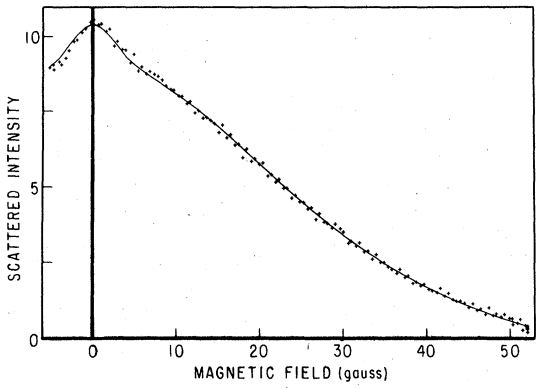

FIG. 10. Decoupling data for the $2\,^2P_{1/2}$ state of ^{6}Li using σ^+/σ^+ polarization. Since the doublet separation is too small to allow easy removal at the $2\,^2P_{3/2}$ fluorescence, the curve displays a kink near zero field due to the $J = \frac{3}{2}$ state (it occurs at lower field since $A_{3/2}$ is somewhat smaller than $A_{1/2}$).

$A_{1/2} = 49.914 \pm 0.025$ MHz (Orth *et al.*[25]) and $(\Delta H)_{av} = 7.5916 \pm 0.0164$ G (obtained from Brog *et al.*). Solving for the interaction constants yields, for the ^{7}Li $2\,^2P$ state, $a_{d3/2} = -1.975 \pm 0.022$ MHz, $a_{o3/2} = 8.311 \pm 0.30$ MHz, and $a_{c3/2} = -9.284 \pm 0.22$ MHz.

The experimental parameters for the $3\,^2P$ state are $A_{3/2} = -1.036 \pm 0.016$ MHz (this work), $A_{1/2} = 13.7 \pm 1.2$ MHz (this work), and $(\Delta H)_{av} = 2.2547 \pm 0.0027$ G (obtained from Isler *et al.*).[24] The interaction constants are, for the ^{7}Li $3\,^2P$ state, $a_{d3/2} = -0.539 \pm 0.267$ MHz, $a_{o3/2} = 2.606 \pm 0.40$ MHz, and $a_{c3/2} = -3.103 \pm 0.668$ MHz.

In calculating the quadrupole moment (below), the values of $\langle r^{-3} \rangle$ are of interest. For the $3\,^2P$ state, these are obtained from the above data substituted into Eqs. (10). For the ^{7}Li $3\,^2P$ state, $\langle r^{-3} \rangle_d = 0.019 \pm 0.009$ a.u., $\langle r^{-3} \rangle_o = 0.019 \pm 0.003$ a.u., and $\langle r^{-3} \rangle_c = 0.045 \pm 0.010$ a.u.

E. Quadrupole moment of ^{7}Li

The quadrupole moment can be obtained from Eq. (17) if $\langle r^{-3} \rangle_q$ is known. Ordinarily, because of the configuration interactions, there is no reason to believe that $\langle r^{-3} \rangle_q$ is exactly equal to either $\langle r^{-3} \rangle_o$ or $\langle r^{-3} \rangle_d$. There are three possible resolutions to this dilemma. The first approach is based upon the fact that the errors associated with $\langle r^{-3} \rangle_o$ and $\langle r^{-3} \rangle_d$ are much greater than their difference. This suggests that, for the purpose of calculating the quadrupole moment only, one can use the two parameter theory (see Ref. 1) and assume that all the $\langle r^{-3} \rangle$ factors (except $\langle r^{-3} \rangle_c$) are equal. Of course, one must use the error associated with the least accurate $\langle r^{-3} \rangle$ in estimating the error of Q. The result is, for the

^{7}Li quadrupole moment, $Q = -58 \pm 26$ mb (method 1), where a Sternheimer correction,[26] R, of 0.012 has been applied.

The other two approaches utilize the theoretical calculations. The second method is based upon the fact that the theoretical ratio $\langle r^{-3}\rangle_o/\langle r^{-3}\rangle_q$ is fairly independent of the principal quantum number for the $2\,^2P$, $3\,^2P$, and $4\,^2P$ states of ^{7}Li (see Ref. 8, Table VII). Following Lunell,[8] we assume that, as the errors are principally systematic, the constancy of this theoretical ratio will hold for highly accurate treatments. Thus, without too large an error, we can obtain $\langle r^{-3}\rangle_q$ for the $3\,^2P$ state by dividing the experimental $\langle r^{-3}\rangle_o$ by the $2\,^2P$ state ratio (which is presumed to be fairly accurate). From Ref. 8, we estimate the ratio as 1.12 ± 0.05. If this is done, the result is, for the ^{7}Li quadrupole moment; $Q = 59 \pm 11$ mb (method 2). Finally, we can use the theoretical values of $\langle r^{-3}\rangle_q$ directly to obtain Q from Eq. (17). Choosing the most recent calculation (Garpman *et al.*[9]) the result is, for the ^{7}Li quadrupole moment, $Q = 59 \pm 8$ mb (method 3), where we have given the theoretical $\langle r^{-3}\rangle_q$ an error of 10%.

VI. DISCUSSION OF RESULTS

Summaries of most published experimental and theoretical values of the parameters that we have measured appear in Tables I–V. In comparing our results to those of other investigators, it should be noted that our method differs fundamentally from that of others in that we measure A_J directly by curve fitting to unmodulated (undifferentiated) curves of fluorescent intensity versus magnetic field. Only one other level crossing experiment on lithium uses curve fitting (Isler *et al.*[24]). All other lithium measurements, however, employ field modulation, which results in experimental curves which are the first derivatives with respect to the field. We deliberately avoided this technique for lithium measurements since any modulation-induced distortion would very likely lead to systematic errors that would be especially troublesome for lithium, as the level crossings are poorly resolved.

Experimental and theoretical lifetime data are summarized in Table I. For the $2\,^2P$ state, we are in essential agreement with most other calculated and measured values of the lifetime. The $3\,^2P$-state lifetimes, however, exhibit a fairly wide variation. The difficulty with the $3\,^2P$-state theoretical lifetimes probably arises from the lack of sophistication of the wave functions used in the calculation. The 10% disagreement between our $3\,^2P$-state lifetime and the most recent other experimental value (Isler *et al.*[24]) is unexplained.

Tables II and III give the calculated and measured values of $A_{1/2}$ and $A_{3/2}$ for the $2\,^2P$ and $3\,^2P$ states of ^{7}Li. Our value of $A_{3/2}$ for the $2\,^2P$ state is in reasonable agreement with that of Orth *et al.*,[25] which one would expect to be the most accurate measurement to date. We are also in good agreement with the results (Lyons and Das[15]) of the reanalysis of the Brog *et al.*[23] level-crossing data. The directness with which we have obtained our $A_{3/2}$ for the $2\,^2P$ state demonstrates one of the main advantages of our method, namely, the lack of ambiguity of the experimental result. Our result did not depend on such theoretical questions as the number of independent hyperfine parameters that need to be measured.

TABLE I. Summary of the experimental and theoretical lifetimes τ for the $2\,^2P$ and $3\,^2P$ states of ^{7}Li.

	τ (10^{-9} sec)	Technique	Year	Ref.
$2\,^2P$	27.2	Bates-Damgaard	1961	28
	26.9(1)	Hartree-Fock	1967	29
	31.9	Exponential decay	1967	30
	27.2(4)	Level crossing	1967	23
	26.4(8)	Level crossing	1972	This work
	26.5	Spin-optimized self-consistent-field	1973	8
$3\,^2P$	202	Hook method	1931	31
	209	Bates-Damgaard	1961	28
	235	Exponential decay	1967	30
	232	Hartree-Fock	1967	29
	182(6)	Level crossing	1969	24
	203(8)	Level crossing	1972	This work
	224	Spin-optimized self-consistent-field	1973	8

TABLE II. Comparison of A_J values obtained by theoretical and experimental workers for $2\,^2P$ term of ^{7}Li.

	$A_{1/2}$ (MHz)	$A_{3/2}$ (MHz)	Technique	Year	Ref.
Expt.	46.17(35)		ODR[a]	1965	21
		−3.36(30)	LC[b]	1966	32
		−3.40(23)	LC	1967	23
		−3.077(30)	[c]	1970	15
		−2.95(4)	LC	1972	This work
	45.914(25)	−3.055(14)	ODR		25
Theor.	32.4	−6.5	RHF[d]	1961	1
	43.1	−4.2	SPHF[e]	1961	1
	45.7	−6.24	CI[f]	1967	2
	45.86	−2.79	BG[g]	1969	3
	42.4	−3.5	SO-SCF[h]	1969	4
	46.0383	−3.0291	Variational BG	1970	5
	44.4	−4.3	UHF[i]	1970	6
	46.021	−3.064	Variation	1973	7
	42.3	−3.3	SO-SCF	1973	8

[a] Optical double resonance.
[b] Level crossing.
[c] Reanalysis of level-crossing work of Ref. 8.
[d] Restricted Hartree-Fock.
[e] Spin-polarized Hartree-Fock.
[f] Configuration interaction.
[g] Bruckner-Goldstone method.
[h] Spin-optimized self-consistent-field.
[i] Unrestricted Hartree-Fock.

Our measurement of $A_{3/2}$ for the $3\,^2P$ state of ^{7}Li is seen to be about 7% larger than the other two measurements that appear in Table III. This discrepancy is particularly distressing as the other two measurements agree with each other yet were done quite differently. One (Budick *et al.*[18]) was done at high field and the other (Isler *et al.*[24]) was the result of a curve fit to low-field, modulated data. The discrepancy is unexplained.

Table IV lists experimental and theoretical results for a_c, a_d, and a_o for the $2\,^2P$ and $3\,^2P$ states of ^{7}Li. For the $2\,^2P$ state, the close agreement among the last three entries suggests that they are very probably correct as they were all done using different methods (two theoretical and one experimental). It is interesting to note that our derived parameters differ from those obtained by Das and Lyons[15] by about 4%, while one of our input parameters $[(\Delta H)_{av}]$ is the same and another

TABLE III. Comparison of A_J values obtained by theoretical and experimental workers for $3\,^2P$ term of ^{7}Li.

	$A_{1/2}$ (MHz)	$A_{3/2}$ (MHz)	Technique[a]	Year	Ref.
Expt.	13.5(2)	−0.96(13)	LC	1966	32
		−0.965(26)	LC	1969	24
	13.7(1.2)	−1.036(16)	D[b] and LC	1972	This work
Theor.	12.9	−1.26	SPHF	1968	10
	12.9	−1.21	SO-SCF	1969	4
	13.0	−1.3	SPHF	1973	8
	13.3	−1.33	UHF	1973	8
	12.9	−1.16	SO-SCF	1973	8

[a] See Table II for explanation of abbreviations.
[b] Decoupling.

TABLE IV. Summary of experimental and theoretical values of a_c, a_o, and a_d for $2\,^2P$ and $3\,^2P$ states of ^{7}Li (all data are in MHz).

	$a_{c3/2}$	$a_{o3/2}$	$a_{d3/2}$	Technique [a]	Year	Ref.
$2\,^2P$	−9.5698	8.6738	−1.8946	BG	1969	3
	−9.888	8.728	−1.869	Variational BG	1970	5
	−10.681	8.091	−1.749	UHF	1970	6
	−9.806(117)	8.638(39)	−1.909(34)	b	1970	15
	−9.371(110)	8.396(57)	−1.975(22)	LC	1972	This work
	−9.963	8.754	−1.855	Variation	1973	7
	−9.838(48)	8.659(37)	−1.876(12)	ODR	1975	25
		8.743	−1.864	Modified many-body theory	1975	9
$3\,^2P$	−3.166	2.436	−0.488	SO-SCF	1969	4
	−3.10(67)	2.61(40)	−0.54(27)	LC	1972	This work
	−3.115	2.442	−0.489	SO-SCF	1973	8
	−2.975(60)	2.577(50)	−0.567(20)	c	1973	8
		2.578	−0.552	Modified many-body theory	1975	9

[a] See Table II for explanation of abbreviations.
[b] Reanalysis of level-crossing data of Ref. 23.
[c] Reanalysis of level-crossing data of Ref. 24.

($A_{1/2}$) differs by less than 1%. This suggests that the source of the discrepancy is the roughly 4% difference between our input $A_{3/2}$ and Das and Lyons'[15] derived $A_{3/2}$. Since Das and Lyons'[15] results are within 1% of the last three in the table, our value of $A_{3/2}$ is probably in error by about 4%. This is somewhat outside the random error of 0.04 MHz for our value of $A_{3/2}$; it might possibly be due to some ignored systematic effect.

Our results for a_c, a_d, and a_o for the $3\,^2P$ state of ^{7}Li are in quite good agreement with the recent calculation by Garpman *et al.*[9] and the reanalysis by Lunell[8] of the data of Isler *et al.*[24] However, our random errors are quite large; this is due mainly to the 10% error in our $A_{1/2}$ input parameter and the fact that our results are obtained by linearly combining fairly large input parameters to obtain somewhat smaller resulting numbers.

Quadrupole interaction data appear in Table V. The only other $3\,^2P$-state quadrupole interaction constant B, with which we can compare our result is that obtained by Isler *et al.*[24] We can, however, scale the $2\,^2P$- state results of Orth *et al.*[25] by the theoretical ratio of $\langle r^{-3}\rangle_q$ for the $3\,^2P$ state to $\langle r^{-3}\rangle_q$ for the $2\,^2P$ state. Using the calculation of Garpman *et al.*,[9] the result is $B(3\,^2P) = -0.066(9)$ MHz, where we have given the theoretical ratio at 10% error. Our value of B is thus about five times larger than that obtained by Isler *et al.* and about 50% larger than

TABLE V. Summary of experimental B values obtained by various workers for the $2\,^2P$ and $3\,^2P$ states of ^{7}Li.

	B (MHz)	Q(derived) (mb)	Technique [a]	Year	Ref.
$2\,^2P_{3/2}$	−0.18(12)	−30(20)	LC	1967	23
	−0.221(29)	−41(6)	ODR	1975	25
$3\,^2P_{3/2}$	−0.019(22)	−11(12)	LC	1969	24
	−0.094(10)	−58(26)	LC	1972	This work [b]
		−59(11)	LC	1972	This work [c]
		−59(8)	LC	1972	This work [d]

[a] See Table II for an èxplanation of the abbreviations.
[b] Q calculated using method 1 (see text).
[c] Q calculated using method 2.
[d] Q calculated using method 3.

the scaled result of Orth *et al.*[25]

Quadrupole moments can be obtained from B in essentially two ways. One can obtain $\langle r^{-3}\rangle_q$ either from the magnetic hyperfine data or from a theoretical calculation. (In this respect, our method 1 is essentially the same as our method 2.) We have found that both approaches yield approximately the same value for Q; this was also the experience of Orth *et al.*[25] The main difference among our different methods of deriving Q is the vastly different associated errors. The theoretical $\langle r^{-3}\rangle_q$ contributes much less to the error of Q than the rather imprecise value of $\langle r^{-3}\rangle_q$ that we have obtained from our magnetic hyperfine data. The only other experiments from which one can obtain Q are the molecular beam experiments which measured the hyperfine structure of LiF and LiH. The quadrupole moment can then be derived from a rather elaborate calculation of the electric field gradient at the nucleus. A typical result for LiH is the calculation by Kahalas *et al.*[27] which yields a value of 43(4) mb for Q.

ACKNOWLEDGMENTS

We are indebted to John Sierssen and Joe Robertson for their fine machining of the apparatus used in these experiments, to Israel Beller for his excellent draftsmanship, and to James Clendenin for his considerable help with the computer programming for the data analysis for this experiment. This work was supported in part by the Joint Services Electronics Program (U. S. Army, U. S. Navy, and U. S. Air Force) under Contract No. DAAG 29-77-C-0019.

APPENDIX: EXPLICIT FORMULA FOR $P_{1/2}$ FLUORESCENCE

Since the Hamiltonian can be easily diagonalized for a $P_{1/2}$ state, the formula for resonance fluorescence [Eq. (1)] can be written in a closed form. The result of a rather tedious calculation is

$$R = 2I + \cos\theta_1\cos\theta_2 + \cos\theta_1\cos\theta_2 \sum_{m=-(I-1/2)}^{I-1/2} \frac{1}{w^2+v^2}\left(w + \frac{v^2}{1+q(w^2+v^2)}\right)$$
$$+ \sin\theta_1\sin\theta_2 \sum_{m=-I}^{I}\left(\frac{(1+\frac{1}{2}qv^2+\frac{1}{8}q)\cos(\phi_1-\phi_2)}{1+q(w^2+v^2)+\frac{1}{4}q^2(w-m)^2} + \frac{q^{1/2}[w(1+\frac{1}{4}q)-\frac{1}{4}qm]\sin(\phi_1-\phi_2)}{1+q(w^2+v^2)+\frac{1}{4}q^2(w-m)^2}\right), \tag{18}$$

where I is the nuclear spin, θ_1, ϕ_1 and θ_2, ϕ_2 are the polar angles of the electric field vectors of the incident and scattered radiation, respectively, and the quantities w, v, and q are defined as follows:

$$w = m + (I+\tfrac{1}{2})x,$$

where $x = g_J\mu_0 H/A(I+\tfrac{1}{2})$,

$$v^2 = (I+\tfrac{1}{2})^2 - m^2,$$

and

$$q = (2\pi A_{1/2}\tau)^2$$

(τ is the lifetime and the magnetic field H is along the polar axis).

In deriving this result, the nuclear Zeeman effect has been ignored; it can be shown that the fractional error in neglecting this interaction is $(1+g_I\mu_I H/A_{1/2})^2$. The first summation in Eq. (18) describes the decoupling effect and the second summation describes the Hanle effect.

*Present address: Dept. of Physics, University of Washington, Seattle, Wash. 98195.

[1]D. A. Goodings, Phys. Rev. 123, 1706 (1961).

[2]R. W. B. Ardill and A. L. Stewart, Proc. Phys. Soc. Lond. 92, 296 (1967).

[3]J. D. Lyons, R. T. Pu, and T. P. Das, Phys. Rev. 178, 103 (1969); 186, 226 (1969).

[4]Robert C. Ladner and William A. Goddard, III, J. Chem. Phys. 51, 1073 (1969).

[5]R. K. Nesbet, Phys. Rev. A 2, 661 (1970).

[6]S. Larsson, Phys. Rev. A 2, 1248 (1970).

[7]T. Ahlenius and S. Larsson, Phys. Rev. A 8, 1 (1973).

[8]Sten Lunnell, Phys. Rev. A 7, 1229 (1973).

[9]Sten Garpman, Ingvar Lindgren, Johannes Lindgren, and John Morrison, Phys. Rev. A 11, 758 (1975).

[10]W. A. Goddard, III, Phys. Rev. 176, 106 (1968).

[11]P. A. Franken, Phys. Rev. 121, 508 (1961).

[12]M. E. Rose and R. L. Carovillano, Phys. Rev. 122, 1185 (1961).

[13]R. Gupta, S. Chang, and W. Happer, Phys. Rev. A 6, 529 (1972).

[14]K. H. Liao, L. K. Lam, R. Gupta, and W. Happer, Phys. Rev. Lett. 32, 1340 (1974).

[15]J. D. Lyons and T. P. Das, Phys. Rev. A 2, 2250 (1970).

[16]R. W. Schmieder, thesis (Columbia University, 1969)

(unpublished).
[17]M. Nagel and F. E. Haworth, Am. J. Phys. 34, 553 (1966).
[18]B. Budick, R. Novick, and A. Lurio, Appl. Opt. 4, 229 (1965).
[19]H. Kretzen, thesis (Hannover, 1968) (unpublished).
[20]W. E. Wentworth, J. Chem. Educ. 42, 96 (1965).
[21]G. J. Ritter, Can. J. Phys. 43, 770 (1965).
[22]W. Happer and E. B. Saloman, Phys. Rev. 160, 23 (1967).
[23]K. C. Brog, T. Eck, and H. Wieder, Phys. Rev. 153, 91 (1967).
[24]R. C. Isler, S. Marcus, and R. Novick, Phys. Rev. 187, 76 (1969).
[25]H. Orth, H. Ackermann, and E. W. Otten, Z. Phys. A 273, 221 (1975).
[26]R. M. Sternheimer and R. F. Peierls, Phys. Rev. A 3, 837 (1971).
[27]S. L. Kahalas and R. K. Nesbet, J. Chem. Phys. 39, 529 (1963).
[28]O. S. Heavens, J. Opt. Soc. Am. 51, 1058 (1961).
[29]A. W. Weiss, Astrophys. J. 138, 1262 (1963).
[30]J. Buchet, A. Denis, J. Desesquelles, and M. Dufay, C. R. Acad. Sci. B (Paris) 265, 471 (1967).
[31]A. N. Filipov, Z. Phys. 69, 526 (1931).
[32]B. Budick, H. Bucka, R. J. Goshen, A. Landman, and R. Novick, Phys. Rev. 147, 1 (1966).